Publications of the Astronomical Society of the Pacific
106: 780–797, 1994 July

Supernova Remnants and the Physics of Strong Shock Waves

DONALD C. ELLISON AND STEPHEN P. REYNOLDS

Department of Physics, North Carolina State University, Raleigh, North Carolina 27695-8202
Electronic mail: don_ellison@ncsu.edu, steve_reynolds@ncsu.edu

KAZIMIERZ BORKOWSKI

Department of Astronomy, University of Maryland, College Park, Maryland 20742
Electronic mail: kazik@astro.umd.edu

ROGER CHEVALIER

Department of Astronomy, University of Virginia, Charlottesville, Virginia 22903
Electronic mail: rac5x@virginia.edu

DONALD P. COX

Department of Physics, University of Wisconsin, Madison, Wisconsin 53706
Electronic mail: cox@wisp.physics.wisc.edu

JOHN R. DICKEL

Astronomy Department, University of Illinois, Urbana, Illinois 61801
Electronic mail: johnd@sirius.astro.uiuc.edu

RYSZARD PISARSKI

NASA/Goddard Space Flight Center, Greenbelt, Maryland 20771
Electronic mail: rlp@ros5.gsfc.nasa.gov

JOHN RAYMOND

Center for Astrophysics, 60 Garden Street, Cambridge, Massachusetts 02138
Electronic mail: raymond@cfassp37.harvard.edu

STEPHEN R. SPANGLER

Department of Physics and Astronomy, University of Iowa, Iowa City, Iowa 52242
Electronic mail: srs@vesta.physics.uiowa.edu

HEINRICH J. VÖLK

Max-Planck-Institut für Kernphysik, Postfach 10 39 80, 6900 Heidelberg 1, Germany
Electronic mail: vlk@vampi.mpi-hd.mpg.de

JOHN P. WEFEL

Department of Physics and Astronomy, Louisiana State University, Baton Rouge, Louisiana 70803-4001
Electronic mail: wefel@phepds.dnet.nasa.gov

Received 1994 February 22; accepted 1994 April 26

ABSTRACT. This paper reports on a *Workshop on Supernova Remnants and the Physics of Strong Shock Waves* hosted by North Carolina State University at Raleigh, North Carolina, September 16–18, 1993. The workshop brought together observers, shock theorists, cosmic-ray specialists, and simulators to address the role supernova remnants can play in furthering our understanding of the complex plasma physics associated with collisionless shocks and particle acceleration. Over fifty scientists presented papers on various aspects of supernova remnants. In lieu of a proceedings volume, we present here a synopsis of the workshop, in the form of brief summaries of each workshop session.

1. INTRODUCTION

When a star explodes and becomes a supernova it deposits its $\sim 10^{51}$ ergs of energy into the interstellar medium in the form of one to several solar masses of material moving at speeds of order 5,000–10,000 km s^{-1}. It may be tens of thousands of years before the blast-wave velocity drops below 200 km s^{-1} and the shock becomes dominantly radiative. Before this time, the remnant is a bright emitter of nonthermal synchrotron radio emission and thermal X-ray emission; where the shock encounters denser clouds, it may be locally radiative and produce bright optical emission. Even if the shock is still adiabatic everywhere, faint Balmer emission may be seen. The physics of these extremely strong shock waves is not well understood, since the shock strengths far exceed anything reproducible in a terrestrial laboratory or observed in the heliosphere. In typical interstellar conditions, the upstream sound speed and Alfvén speed are roughly comparable at 10–100 km s^{-1}, so that even when radiative, a supernova remnant (SNR) shock may have a Mach number of 10 or greater, and the historical remnants of the last millennium have shocks with Mach numbers in

the range 10–300. Shocks this strong, accompanied by such a plethora of observational information, are difficult to find anywhere else in astrophysics and may, in fact, be the strongest shocks in nature.

The workshop was divided into six sessions, more or less by topic, covering three full days. Each session consisted of six or seven oral presentations plus poster papers, and was reviewed by two rapporteurs.

The sessions and corresponding rapporteurs were

(1) Thermal X Rays. Borkowski and Pisarski
(2) SNR Morphology: Hydrodynamics and Radio Observations. Chevalier and Dickel
(3) Relativistic Shocks, Simulations, and Diverse Observations. Spangler and Ellison
(4) Cosmic Rays and Acceleration to High Energies. Völk and Wefel
(5) Shock Precursors and Optical Observations. Cox and Raymond
(6) Cosmic-Ray Electrons and Propagations. Völk and Reynolds

We have revised the original sessions somewhat, since we are no longer constrained to have equal-length sessions. Session 4 (Sec. 5 below) now contains all discussion related to cosmic rays except for cosmic-ray electrons; three papers on this subject remain in Session 6 (Sec. 7 below), reviewed by Reynolds. In Session 4, authors of subsections are indicated; otherwise, contributions were written jointly by the corresponding rapporteurs. The reports differ somewhat in depth of coverage and extent of editorializing, according to the predilections of the authors, whose responsibilities should not be considered to extend beyond the bounds of their sessions. The reports were combined and lightly edited by S.P.R. and D.C.E., who supplied the introductory material and the Summary.

Most reports assume a background in astrophysical shock waves, SNRs, and particle acceleration. Useful reviews on those subjects include Axford (1991) on cosmic rays; Draine and McKee (1993) on the general theory of interstellar shocks; Drury (1983), Blandford and Eichler (1987), and Jones and Ellison (1991) on shock acceleration; Raymond (1991) on shock precursors; and Reynolds (1988) and Roger and Landecker (1988) on SNRs.

2. THERMAL X RAYS

2.1 Introduction

X-ray emission provides the most direct and fundamental knowledge about the state of the shocked gas in supernova remnants (SNRs). Its diagnostic values are many: X-ray intensity depends quadratically on the gas density, X-ray spectra are sensitive to electron temperatures, gas abundances and SNR ages, and X-ray morphology presents us with information on the SNR structure.

The major problem with using X-ray observations as the diagnostic of hot shocked plasmas has been the modest spectral and spatial resolution of X-ray satellites. This problem is being addressed by new observatories such as *ROSAT* and *ASCA*. This development could be seen at this workshop: most contributions concentrated around new, high-quality data, mainly from the *ROSAT* satellite.

2.2 New Observations

The Cygnus Loop, a large (~3° diameter), nearby SNR, was the subject of two studies. *Decourchelle and Sauvageot* have observed the northern portion (~1° in size) with the *ROSAT* proportional counter in the energy band 0.1–2 keV. The authors explored whether an X-ray bright feature which resembles a "V" is a bow-shock structure or a geometrical projection effect. They mapped both sides of the "V" in the light of [Fe X] λ6374 and found that the left arm of the "V" is redshifted while the right arm is blueshifted. This led them to conclude that these two arms are independent and that this structure is caused by geometrical projection.

Decourchelle and Sauvageot found temperature variations across the whole field of view of their observation. In general the "V" shaped structure and the shock ahead of this "V" were cooler than the northeast (NE) region. The authors obtained the best spectral fits using a two-temperature Raymond–Smith (RS) equilibrium ionization plasma model (nonequilibrium ionization models did not improve the fits). The "warm" temperature varied from 0.05 to 0.16 keV while the "hot" temperature varied from 0.245 to 0.8 keV over the whole field of view. The NE region was broken up into nine fields in order to study the SNR from the shock towards the interior. The hot temperature showed large variation (0.3–0.6 keV) peaking at the sixth field in from the shock while the warm component was uniform.

The *ROSAT* High Resolution Imager (HRI) (field of view ~40′) was used by *Levenson* et al. to observe a small isolated cloud in the southeast region of the Cygnus Loop. This cloud is located to the apex of a large-scale indentation of the X-ray shells; previous interpretations explain this as a small isolated cloud that has been engulfed by the blast wave. The authors argue that this morphological interpretation is not accurate based on the better *ROSAT* and optical data. While there is a strong correlation between optical and X-ray emission, the situation appears to be more complex, with projection effects being of primary importance.

Shell-like SNRs, in both radio and X-rays, are thought to be the natural outcome of a supernova explosion in a uniform medium, in the absence of a central pulsar. This implies that barring absorption effects, any SNR dominated by centrally located thermal emission must contain a pulsar, or that our ideas about the evolution of SNR X-ray morphology are incorrect. Centrally filled SNRs were of considerable interest at this meeting. *Seward and Velusamy* presented *ROSAT* observations of Kes 79. This remnant is dominated by a bright and clumpy interior X-ray emission, surrounded by a faint outer shock. On the basis of a low-energy cutoff seen in the *ROSAT* data, the authors argued for a 5 kpc distance to the remnant, half that previously suggested. The authors then estimated a total X-ray emitting mass of $7.8M_{\odot}$, SNR age of 2500 yr, and a low supernova ejecta kinetic energy of 6×10^{49} ergs. Of particular interest are centrally located, X-ray emitting clumps with a total mass of $3.3M_{\odot}$. Similar

centrally filled SNRs were discussed by *Dickel*. Two notable examples are W 49B and HB 9, where X-ray emission is located well within the radio emission contours.

Two somewhat similar remnants, CTB 109 and IC 443, were observed by *Rho, Petre, and Hester* with the *ROSAT* Position Sensitive Proportional Counter (PSPC). CTB 109 is a composite that consists of a radio shell and a partial eastern X-ray shell surrounding an X-ray bright pulsar with an apparent X-ray emitting "jet." No X-ray shell is visible on the western side due to the interaction of the SNR with a molecular cloud. IC 443 has an optical and radio shell while the X-ray emission is peaked inside the radio shell. The authors claim that the mosaicked observations reveal a new SNR $\sim 1°$ east of IC 443 which includes this SNR's eastern arm. This X-ray object forms a complete shell ($\sim 1°$), part of which passes through a band of low X-ray brightness associated with IC 443.

The jetlike feature in CTB 109 has a thermal spectrum with no evidence of synchrotron radiation. A two-temperature (0.13 and 0.3 keV) RS model provides the best fit to the "jet" spectrum. A one-temperature RS model (0.24–0.33 keV) provides the best fit for the shell (excluding pulsar and "jet"). The absorbing column density decreases from north to south as does the photon energy. A CO (carbon monoxide) arm is observed to extend towards the eastern shell (above the pulsar). This CO region, where X rays are faint, has lower column density than the surrounding jetlike feature, indicating the lack of X rays is not due to absorption. It may be caused by the molecular cloud and shock interaction: as the shock crosses the clouds, it becomes radiative and emits fewer X rays.

IC 443 was also fit using a two-temperature RS model where the low-temperature component varied from 0.1–0.25 keV and the hot component had a range of 0.4–0.7 keV over the whole remnant. The absorbing column density varies and its distribution is largely consistent with the CO map of the local molecular cloud, according to the authors. They also find that a band of low X-ray brightness bisecting the bright NE region has lower column density and different temperatures from neighboring regions. One way to explain this is to propose a second SNR as a foreground object that would have a different temperature and absorbing column.

Edgar et al. presented the first spectrum of the soft X-ray background obtained with a Shuttleflown Diffuse X-ray Spectrometer in the energy range 150–300 eV. The spectrum was taken along a 150° strip along the Galactic plane. As expected, the spectrum is dominated by emission lines, the strongest of them identified with a S VIII line. However, the spectrum cannot be fit with isothermal (10^6 K) models with normal (cosmic) abundances. A much better agreement is obtained when $\sim 50\%$ of Mg, Si, and Fe are assumed to be depleted onto dust grains. This is the first evidence for the depletion of refractory elements based on an X-ray spectrum from a hot astrophysical plasma. A satisfactory fit to the spectrum of the diffuse X-ray background also requires an additional temperature component with $\log T \approx 6.4$.

2.3 Theoretical Implications

The first impression given by new observations is of complex morphologies, differing substantially from idealized theoretical constructs used in modeling of SNRs. Then, a question arises as to whether SNRs evolve in accordance with our current understanding of a supernova explosion in a uniform medium or whether a substantial modification of this scenario is necessary. The latter possibility was suggested by *Dickel* who noted that while young and old SNRs have a characteristic shell structure in X rays, centrally peaked X-ray emission is often seen in middle-aged SNRs. Continuing studies of *ROSAT* data on SNRs, coupled with theoretical efforts, should provide an answer to this and related questions about SNR structure and evolution.

The necessity of renewed theoretical efforts was amply demonstrated by two contributions on theoretical modeling of Kepler's SNR. The X-ray spectrum of Kepler's SNR is dominated by strong Si and S lines, and a strong Fe Kα complex. On the basis of this Fe complex strength and with the help of relatively simple models, previous investigators concluded that the Fe abundance is substantially above solar and attributed this to the Fe production in the supernova explosion. In order to investigate this intriguing possibility, *Decourchelle and Ballet* presented an extensive set of X-ray modeling calculations based on analytic self-similar solutions appropriate for a young SNR. They confirmed that enhanced abundances of heavy elements within the supernova ejecta can indeed explain existing X-ray spectra. Their analysis points to a massive supernova progenitor, in agreement with the presence of a dense circumstellar medium around this high-latitude remnant. A somewhat different approach was taken by *Borkowski, Sarazin, and Blondin* who used their two-dimensional hydrodynamic simulation based on a bow-shock model of Bandiera, again involving a massive supernova progenitor. Using a newly developed technique for X-ray emission calculations in two-dimensional hydrodynamic simulations, they calculated an X-ray spectrum and compared it with observations. In contrast to other investigators, they found only a modest (50% above solar) Fe overabundance and attributed this result to the presence of a circumstellar medium shell in their models.

The Kepler's SNR modeling efforts once again demonstrate that X-ray emission strongly depends on a remnant's structure. In view of complex morphologies revealed by *ROSAT* observations and with incoming high-quality spectral observations with the *ASCA* satellite, renewed theoretical efforts aimed at modeling X-ray emission become timely and relevant. In particular, it is hard to understand morphologies of SNRs within the framework of simple one-dimensional spherically symmetric models. X-ray emission calculations based on two- and three-dimensional hydrodynamic simulations are necessary for that purpose. Proper care is also required to assure that all relevant processes are taken into account. For example, the spectra of the diffuse X-ray background presented by *Edgar* et al. show evidence that elements such as Mg, Si, and Fe are partially locked in dust grains. Because dust is present in SNRs, X-ray modeling efforts should take this important effect into account.

2.4 Future Prospects

New high-quality X-ray observations presented at this meeting mark a beginning of a new era in SNR research. *ROSAT* observations of SNRs are just beginning to be analyzed, and spectral observations are being gathered by the *ASCA* satellite. The results presented at this meeting indicate that these new data are providing qualitatively new information which in many cases cannot be explained within the framework of existing theoretical models. Once these data are analyzed and interpreted, a new, more complete picture of SNRs will emerge.

To take advantage of this observational breakthrough, intensive theoretical efforts in X-ray emission modeling appear necessary. It will generally be required to extend one-dimensional modeling to two or three dimensions with the help of hydrodynamic simulations. Initial efforts in this direction are described below (Sec. 3.1). Models should also properly take into account important physical processes such as the depletion of heavy elements onto dust grains.

With these new observations and with supporting theoretical efforts, there is finally a good prospect of addressing basic questions related to the physics of strong collisionless shocks. The most fundamental question relates to the collisionless electron heating in strong shocks. As demonstrated by modeling of Kepler's SNR presented by *Borkowski* et al., it is possible to find the amount of collisionless electron heating in young SNRs from their X-ray spectra. Because thermal electrons might be important as seed particles for electron acceleration in SNRs, the collisionless electron heating was of much interest at this meeting. Another relevant issue is the influence of relativistic particles and magnetic fields on shock jump conditions. These jump conditions (and X-ray emission) will be different if a substantial transfer of kinetic energy into the relativistic component were to take place.

3. SNR MORPHOLOGY: HYDRODYNAMICS AND RADIO OBSERVATIONS

3.1 Shock Fronts in Young Remnants

Numerical simulations of the evolution of SNRs have begun to consider multidimensional aspects of the flows. *Blondin* presented two-dimensional hydrodynamic calculations of the early driven-wave (reverse-shock) phase and the transition to the Sedov blast-wave phase. Rayleigh–Taylor-type instabilities develop in the decelerating shell and result in considerable mixing during the transition to the blast wave. *Jun and Norman* have simulated the early instabilities in three-dimensional calculations and found qualitatively similar results to the two-dimensional case, although the unstable fingers of denser ejecta, penetrating into the less dense shocked ISM, grow somewhat longer. The instabilities are expected to amplify the magnetic field and a beginning estimate of the observational implications of these hydrodynamic models has been made by *Jenkins, Blondin, and Reynolds*, who modeled the resulting synchrotron radio emission.

In these models, the strongest radio emission from a remnant like Tycho (Dickel et al. 1991) can be accounted for because it occurs inside of the shock front in a region that is expected to be unstable to these Rayleigh–Taylor modes. The radio polarization suggests a radial mean magnetic field, which is consistent with the radial stretching that might be expected from the motion of the unstable fingers. However, the radial mean magnetic field appears to occur right at the shock front as well as interior to it (*Milne, Strom*). In remnants like Tycho and SN 1006, the radio emission shows a sharp turn-on at the location of Balmer-line optical emission and is also coincident with a sharp turn-on in the X rays. There is little doubt that this is the site of the shock front. There are field fluctuations on a small scale throughout the shell but certainly no tangential alignment is seen at this shock on the leading edge of the shell. At the shock, the component of the magnetic field parallel to the shock front is compressed by the shock compression ratio (probably about 4) while the perpendicular component is unaffected.

It would be possible to obtain an apparently radial magnetic field if the ambient field were directed along the line of sight, but this requires a very special geometry and it is implausible that such a situation would occur for all young SNRs observed with sufficient resolution. The radial field alignment at the shock front also affects another important problem discussed at the workshop: the question of how the relativistic particles actually get accelerated at a shock. *Jokipii* emphasized that quasiperpendicular shocks will produce much higher energies than quasiparallel ones, because the acceleration rate is greater, and the finite age of the remnant limits the energies to which particles can be accelerated (see Sec. 5.5). But if the accelerated particles originate in the thermal background, the enhanced acceleration of quasiperpendicular shocks may be outweighed to some extent by their reduced injection efficiency (see Sec. 4.4).

A plausible solution to the problem of the field orientation and the acceleration is that there is a small-scale instability which randomizes the magnetic field at the shock front together with some radial stretching. The polarization percentage at the shock fronts is relatively small ($<20\%$, where the theoretical maximum for synchrotron radiation is of order 70%) so the magnetic field is probably more random than radial. The nature of the possible instability is not known. *T. Jones* suggested a secondary instability that occurs when a shock is strongly cosmic-ray dominated and there are fluctuations in the preshock medium (Jones and Kang 1993). Cosmic-ray dominated shocks emerge from the two-fluid formalism (see Sec. 5.7) as a class of solutions in which most entropy generation happens in the cosmic-ray component, with a shock thickness set by the cosmic-ray diffusion length rather than the thermal ion gyroradius. In these solutions, no viscous subshock exists to provide thermal-gas heating. However, there is no clear evidence that the shock fronts are cosmic-ray dominated to the required degree, and in fact the presence of strong X-ray emission from a large fraction of all SNRs indicates that their shocks are not cosmic-ray dominated. Our understanding of high Mach-number collisionless shock waves is poor and it may be that plasma instabilities can give the required turbulence. This area is ripe for further research. Current numerical plasma simulations are almost universally done for low Mach numbers (below about 5) so

we know virtually nothing about instabilities in high Mach-number shocks.

3.2 Irregular Structures in Older SNRs

Among the older remnants (ages greater than a few thousand years) are numerous examples of objects with very irregular radio structures (*Roger*). To help investigate these, powerful numerical methods are being brought to bear not only on general SNR evolution, but also on the interaction of blast waves with clouds. Two-dimensional hydrodynamic calculations show that on a time scale of several "cloud-crushing times," a cloud is fragmented by the blast wave and the fragments are accelerated by the flow (Klein et al. 1994). *Mac Low* showed two-dimensional calculations that included a magnetic field along the direction of the blast-wave motion. The magnetic field reduces the generation of vorticity at the cloud surface and thus reduces the amount of fragmentation. Also, the shock acts to focus the magnetic field, bringing it up to equipartition with the post-shock gas; this region is potentially a site of strong synchrotron radiation.

Stone has extended the hydrodynamic and MHD calculations of cloud interaction to three dimensions. In the hydrodynamic case, the addition of the third dimension yields a considerably more complex flow, and fragmentation and mixing are enhanced. In the MHD case, it is possible to calculate the case of a magnetic field perpendicular to the direction of shock motion; the result is strong field amplification, a flattened cloud, and more rapid cloud acceleration. These calculations of shocked clouds have generally assumed an adiabatic gas. For comparison with optical observations, it would be useful to include realistic radiative cooling. The filaments seen in older remnants at optical and radio wavelengths have densities of about 200 particles cm^{-3} and involve radiative shock fronts. Also, many remnants appear to be hitting clouds that are relatively large compared to the blast-wave radius unlike the small clouds assumed in the computations.

The observed structures in older SNRs range from non-round shells through barrel shapes, e.g., 1209-51 (*Roger*), long arcs sweeping out from the shell, e.g., MSH 15-52 (G 320.4-1.2) (*Milne*), to possibly multiple intersecting SNRs, e.g., 3C 400.2 (*Dubner*) and CTB 109 (*Rho*). It is unlikely, however, that two or more remnants will actually touch each other. A typical O-B association might have 20 stars which could become supernovae after lifetimes of perhaps 10^7 yr. With SNR lifetimes of less than 10^5 yr it is therefore unlikely that a supernova would go off close enough to another in a short enough time span for their SNRs to interact. On the other hand, it is quite likely that a supernova can explode in a cavity or wind-blown bubble and/or a remnant can break out into a less dense region carved out by some earlier event. Some chance coincidences along a line of sight, for example, down a Galactic spiral arm, are possible but over 10% of the approximately 150 Galactic SNRs appear to show associated structures, which is a large fraction when the SNRs fill only about 2% of the area of the Galactic plane.

Some of the Milne's polarimetry indicates that the apparent breakouts are often more visible in polarized intensity than in total intensity. The field appears to be dragged out along the direction of expansion and parallel to the walls of the sometimes twisted tunnels through which the breakout progresses. Within individual remnants, the only good example of a tangential magnetic field alignment is in the barrel remnant 1209-51 (*Milne*). Where is the radio emission actually generated in these structures? Is it from material piled up near the walls of the enclosure, is it amplified by turbulent flow through a nozzle, or does the emitting gas from the original SNR just break out to fill the tunnels, bubbles, and other holes in the ISM? Perhaps the three-dimensional MHD code being developed by *Stone* and collaborators can be used to model a situation in which the SN ejecta hit a wall and then penetrate through into an open hole or tube. What are the dynamics, and can the shock and/or turbulence act to increase the radio emission in such a situation? Finally, what do the breakouts tell us about the ISM? If the openings contain the warm medium in *Cox's* newest model, are the density contrasts sufficient to produce the observed structures?

3.3 Summary

It is clear that the calculations and the observations are both reaching the point where a detailed comparison of their results for SNRs will be very fruitful. The observers need to provide more details of the magnetic-field configurations on the size scale of individual filaments, particularly for older remnants, and the theorists need to model the interaction with surroundings having a variety of realistic variations in physical conditions.

4. RELATIVISTIC SHOCKS, SIMULATIONS, AND DIVERSE OBSERVATIONS

4.1 Crab Nebula

Outside the heliosphere, studies of shock acceleration of charged particles to high energy usually concentrate on processes at shocks of shell-type supernova remnants. However, two of the papers in this session, those of *Arons and Harding*, were concerned with particle acceleration by the Crab Nebula. An advantage of studying the Crab is that it is obviously accelerating particles and to quite high energy. Harding reviewed the situation, presenting evidence that photons with energies up to 1000 GeV have a nebular origin. Since this radiation is attributed to synchrotron or inverse-Compton radiation, it tells us that electrons are accelerated to at least these energies. Another advantage of the Crab is that we can fairly clearly see what is going on. Observations showed by *Arons* revealed the wisps close to the Crab pulsar, which are now fairly generally interpreted as shock waves or shock-associated phenomena.

Both Arons and Harding attributed the powerful particle acceleration processes in the Crab to phenomena at the inward-facing shock inside the nebula where the relativistic pulsar wind is shocked, at a radius about 10% of the nebular radius. However, the acceleration processes invoked were vastly different. Arons summarized a now substantial literature produced by himself and his *socii*, essentially a plasma microphysical model. Arons begins by assuming a relativis-

tic wind from the pulsar, composed primarily of electrons and positrons, but with a trace ion component as well. The ionic "fellow travelers" are extremely important to the model. Since the relativistic wind must eventually interact with the stationary interstellar medium, an inner shock must form (this being a fairly general prediction of any wind model). At this inner shock the electrons and positrons are thermalized, converting the directed bulk energy which was in the relativistic wind into thermal energy. This shock thermalization is responsible for much of the X-ray and gamma-ray emission via synchroton radiation, and incidentally the radio synchrotron radiation further out in the nebular. An additional appealing feature is that since one expects this shock to be essentially perpendicular so far from the central pulsar, there is a compressive magnetic-field amplification at the shock, facilitating the production of synchrotron radiation.

While the model of an electron–positron "inner perpendicular shock" satisfies the requirement of a high-energy electron and positron plasma which an produce the requisite X-ray and gamma-ray synchro-Compton radiation, it fails to account for one major feature of the Crab Nebula observations. Observations indicate a power-law electron spectrum extending to high energies. One expects, as is borne out by the computer simulation studies of Hoshino et al. (1992), described below, that the expected particle distribution should be a relativistic Maxwellian. A successful shock model therefore requires some additional "afterburner" to suscitate a power-law tail on the electron (and positron) distribution.

At this point the relativistic protons come into play. The inner shock will form on scales of the electron inertial length. The more massive protons will sail through the electron–positron shock transition, and begin gyromotion in the compressed, post-shock magnetic field. The distribution function of these ions will be a ring distribution which is unstable to the generation of magnetosonic waves. Arons and co-workers have shown that these waves can resonate with the positrons and damp. Arons proposes that the power-law tail of the positrons is produced by a transfer of energy from the unstable, gyrotropic protons, through the magnetosonic waves, and thence to the protons. The analytic theory is exceedingly simple, consisting of a balance between energy radiated in the form of magnetosonic waves and energy radiated by the positrons as synchrotron radiation.

While the analytic theory of the model is clever and appealing, what makes the arguments compelling is the support providing by a computer simulation of the shock using a one-dimensional, electromagnetic particle-in-cell code. In these simulations one can see the formation of the shock on the short electron inertial length, the gyrating protons, the kinetic instability leading to magnetosonic waves, and the damping on the positrons to form a power-law tail. Few astrophysical theories have this level of support. The proposed mechanism also bears considerable microphysical similarity to processes known to operate in the magnetosphere or heliosphere.

Nonetheless, there remain a few concerns which serve perhaps to mute the chorus of Hosannas. The relative number density of protons seems an imponderable, relegated in this theory to the role of an arbitrary parameter. Clearly if one makes the density too large, the shock will form on the ion, rather than electron, inertial scale length, and the whole mechanism will cease to function. If the energy density in protons becomes too small, however, there will clearly not be enough energy to transfer to the magnetosonic waves and thence to the positrons, and it would seem that a prominent power-law spectrum would not occur. Thus the "astrophysically correct" value for the proton to electron/positron ratio does not seem to proceed naturally from the theory.

Another worry is that the computer simulations were carried out with an unphysical proton to electron mass ratio of 20. Arons conjectures that a realistic mass ratio might remove positron favoritism and allow equal energy inputs to electrons and positrons, but this remains to be demonstrated. One can easily speculate about a disruption of the resonant conduit if realistic mass ratios were used. It would seem an easier task to get two species of particles to resonate with the same waves when their mass ratio is 20 than when it is 2000.

The theoretical model of *Harding* also is concerned with the inner shock of the Crab Nebula wind, but invokes Fermi acceleration rather than acceleration by plasma waves. Harding notes that there are objections to the operation of Fermi acceleration based on the fact that the strong magnetic field and highly perpendicular geometry would prevent particles from escaping upstream where they might scatter from incoming irregularities. Harding points out that the magnetic field in the wind would reverse on a scale of $l \simeq c/\Omega$, where c is the speed of light and Ω is the rotation frequency of the pulsar. In the case of the Crab Nebula pulsar, this scale is of the order of few thousand kilometers, or much smaller than the gyroradius of energetic particles. She then suggests that energetic electrons and positrons are able to diffuse substantial distances upstream so as to be accelerated by the Fermi mechanism. Obviously the diffusive acceleration process would still require the presence of plasma turbulence to furnish the scattering. The types of modes which would provide such scattering, and the means by which they would be generated, remain to be specified.

Harding calculated the maximum energy to which shock acceleration could accelerate electrons, this being the usual value at which the Larmor radius equals the shock radius. Again, this value can be readily calculated for the wisps and is of the order of 5×10^{15} eV. The synchrotron lifetime for such particles is of the order of a few months. Since one might expect particle acceleration to be somewhat intermittent near the maximum attainable energy, Harding suggests that variability might be observable at the photon energies corresponding to the maximum electron energies. These photons are gamma rays with energies of order 500 MeV.

An issue raised in the discussion following this paper regarded the form of the magnetic field in the pulsar relativistic wind. The arguments made by Harding require $\langle \mathbf{B} \rangle = 0$ where $\langle\ \rangle$ indicates some suitable temporal or spatial average. The vanishing of this field allows particles to escape far upstream. Arons argued that this was likely to be the case only very close to the pulsar equator, say within a degree or so of latitude. Outside this range there is a systematic component

of the azimuthal magnetic field which becomes larger with increasing latitude, and which would prevent particles from escaping upstream. Arons suggested that observation of the wisps close to the pulsar shows that the acceleration region must in fact extend to pulsar latitudes much higher than a few degrees.

4.2 Vela Supernova Remnant

De Jager presented a paper on multiwavelength studies of the Vela SNR and was able to deduce the presence of a standing oblique shock in the pulsar wind. Using various scaling arguments, De Jager argued that the Crab and Vela pulsars differ in that the Crab may have a strong shock with significant conversion of field energy into particle energy while Vela has a weak (mainly) oblique shock with little conversion of field energy into particle energy. The indication of the presence of an oblique shock follows from the radio polarization measurements, although this is difficult to understand since, from kinematics, a relativistic shock should always appear to be nearly perpendicular in the lab frame. (A parallel shock has the shock normal parallel to the upstream magnetic field, while a perpendicular shock moves across magnetic field lines. An oblique shock is in between, and the obliquity angle θ_{Bn} is the angle between the shock normal and upstream magnetic field.) Furthermore, 0.5° polar extensions from the pulsar are seen as X-ray synchrotron-emitting regions extending into the northeast and southwestern directions. This is evidence of the acceleration of electron/positron pairs to energies $\sim 10^{15}$ eV by the pulsar wind shock in the polar regions. However, even in the polar regions we expect the shock to be transverse (perpendicular) due to the relativistic transformation. Further direct evidence for accelerated electrons in the polar regions comes from the detection of TeV photons offset by 0.2° from the pulsar in the southwest direction. De Jager was also able to reproduce the observed flux of TeV gamma rays by inverting the radio and X-ray spectrum to obtain the electron spectrum in the polar regions, and hence the flux of inverse Compton scattered TeV gamma rays with little freedom in parameters.

4.3 Supernova Remnant Distances

A contribution to the perennial problem of determining supernova remnant distances was made by *Kassim*. A knowledge of the distance to a supernova remnant is necessary for just about any astrophysical inference, but credible distances, even approximate ones, are known for less than 25% of Galactic SNRs. Kassim discussed a simple but clever scheme that definitely merits use by workers in the field, particularly in the case in which there is no alternative distance estimate. Kassim's method relies on two ingredients. First, X-ray observations of the remnant must be available, and of sufficient quality to determine the temperature of the hot interior of the remnant. Second, the method explicitly relies on the assumption that the remnant is in the Sedov phase of SNR evolution. The radius of a Sedov-phase remnant is $R = 14(\epsilon_0/n_0)^{1/5} t_4^{2/5}$ pc where ϵ_0 is the initial blast energy in units of 10^{51} ergs, n_0 is the upstream density in cm^{-3}, and t_4 is the time since the explosion in units of 10^4 yr. Differentiation of the above expression shows that the expansion speed of the remnant also depends on the same quantities of the explosion energy, density of the medium into which the blast wave is propagating, and the time since the explosion. In the general case, none of these quantities is known.

However, X-ray observations which yield a temperature for the interior of the remnant provide a measurement of the expansion speed, since the post-shock temperature is directly related to the expansion speed of the remnant. Furthermore, calibrated observations of the X-ray intensity provide a measurement of the density in the interior of the remnant, which may be related to the upstream density via the Rankine–Hugoniot jump conditions. Thus only the blast energy ϵ_0 prevents a complete solution of the problem. Kassim deals with this by simply *positing* the standard blast-wave energy of $\epsilon_0 = 10^{51}$ ergs, and thus obtaining all of the relevant SNR characteristics, including the distance. One might call the distance obtained in this manner the Sedov distance to a supernova remnant. Kassim clearly recognizes that in reality the blast energy might vary from remnant to remnant. However, the radius and expansion speed of the remnant are only dependent on the one-fifth power of the explosion energy, so a fair amount of variability has relatively little influence on the derived distance, which winds up varying as $\epsilon_0^{2/5}$. What will tend to make SNR astronomers particularly forgiving of this shortcoming is the otherwise complete ignorance of the distance for most remnants.

Kassim then proceeded to discuss the application of this method to several remnants with independently known distances (Kassim et al. 1993). With one exception, the Sedov distance was in quite good agreement with the other distance values. The obvious discomfort which many scientists will have with this method is that it requires fidelity of real supernova remnants to the theoretical ideal of the Sedov solution. This implies not only that the remnant be in the Sedov phase, but that one can speak meaningful of a single external density and interior temperature, and that the X-ray luminosity is well-described by an equilibrium-ionization plasma with cosmic abundances. In addition, the observed X-ray temperature must give the shock velocity, requiring electron–ion equipartition. In the cases of remnants which are the best observed, such as the Cygnus Loop, it is clear the structures are inhomogeneous in every property. Nonetheless, these sobering meditations on reality should in no way preclude adding this technique to the tool kit of SNR astronomers.

4.4 Monte Carlo Simulation of Oblique Shocks

Baring presented an update on the simulation of oblique shocks using a Monte Carlo technique (Baring et al. 1993, 1994). This technique has been shown to be an effective method for calculating the efficiency and spectral characteristics of Fermi particle acceleration in parallel shocks and is now being extended to oblique shocks where the upstream magnetic field makes an angle with the shock normal. Most shocks in nature will be oblique and it is important to understand the effects of obliquity on the injection of thermal particles and the acceleration process in general, and, in particu-

lar, on the acceleration rate. Unfortunately, oblique shocks are more complex than parallel ones because the magnetic field and the associated shock-layer electric field cannot be neglected. In the interaction of particles with the shock layer, both reflection and energization can occur, while in strictly parallel shocks, energization comes solely from scattering between the converging upstream and downstream flows. In addition, cross-field diffusion must be treated explicitly, making it necessary to invoke additional parameters.

Understanding oblique shock acceleration is of fundamental importance for SNRs for several reasons. First, we would like to know if the changes in radio intensity often seen around the edge of shell-type remnants come from a variation in the acceleration efficiency of the relativistic electrons (Reynolds and Fulbright 1990). We cannot as yet measure the upstream magnetic-field orientation, but it is certain to vary around a remnant, demanding a theory that predicts how the intensity of radio emitting electrons varies with θ_{Bn}. Another important reason for investigating oblique shocks comes from the fact that they accelerate particles more rapidly than parallel ones. Jokipii (1987) (see also Decker 1988 and Ostrowski 1988) has pointed out that oblique shocks can have far greater acceleration rates than parallel shocks, as described below (Sec. 5.5). In some cases a factor of 1000 increase can be achieved, with profound consequences for cosmic-ray acceleration in SNRs because the maximum energy that can be produced basically scales with the acceleration rate. If a factor of 1000 is actually achieved, this would solve the long-standing problem (e.g., Lagage and Cesarsky 1983) of obtaining cosmic rays up to the "knee" (i.e., $\sim 10^{15}$ eV) in remnants where the maximum energy is determined by the finite age of the remnant. An additional reason for understanding particle injection at oblique shocks is to determine if there are compositional biases that occur whereby different ion species are injected or accelerated more readily than others.

The basic results that Baring presented showed that while the acceleration rate does indeed increase with θ_{Bn}, there is a corresponding decrease in the number of particles that get injected and become accelerated. This is easy to understand when it is realized that in order for a particle to be Fermi accelerated in an oblique shock, it must either enter the downstream region and then return back upstream, or gyrate in the shock layer, gaining energy in the $\mathbf{u}\times\mathbf{B}$ electric field. Both of these processes depend strongly on the particle energy and the magnetic field orientation and it becomes highly improbable for thermal particles to be accelerated beyond thermal heating in high Mach-number oblique shocks.

However, the problem has not yet been solved, even within the restrictions of the Monte Carlo technique. As mentioned above, cross-field diffusion must be treated properly in oblique shocks and this will have a large effect on the injection rate as well as the acceleration rate. Preliminary results show that there is a trade-off; if cross-field diffusion is strong enough to allow efficient particle injection from thermal energies, the corresponding acceleration rate decreases. If strong turbulence is present, the acceleration rate and injection efficiency tend toward the values for a parallel shock regardless of θ_{Bn}. Additionally, if oblique shocks are indeed efficient accelerators, the nonlinear feedback effects of the accelerated particles on the shock structure must be included self-consistently. Thus far, this has not been done in a model where injection is treated self-consistently, but work is progressing with the Monte Carlo treatment.

If suprathermal particles are available, say from radioactive decay in young SNRs or from quasiparallel portions of the shock, the problems with injection in oblique shocks become less severe and the high acceleration rates may be much more important. This subject is discussed further in Sec. 5.5 below.

4.5 Shock Acceleration of Electrons

Ellison gave a discussion of the problems associated with electron acceleration in shocks. It is an interesting fact that outside the heliosphere there is clear evidence that shocks accelerate electrons (through synchrotron emission) but there is little or no evidence that these shocks accelerate ions, even though most researchers believe they do. This is the case in SNRs as well as extragalactic radio sources. Within the heliosphere, on the other hand, where we have direct spacecraft observations of shocks, we can see the acceleration of thermal ions taking place in good agreement with the Fermi model (e.g., Ellison et al. 1990). However, thermal electrons are not seen to be accelerated at heliospheric shocks even though spacecraft would have seen them if they had been accelerated with efficiencies even a small fraction of the observed ion acceleration efficiency. It is likely that the low Mach number of heliospheric shocks may be the important factor that limits the acceleration of thermal electrons, but we have virtually no understanding of how this takes place and it is likely that an adequate understanding of the problem will only come with full-particle plasma simulations (e.g., Pantellini et al. 1992).

Some interesting things can be said about electron acceleration apart from the injection problem. Reynolds and Ellison (1992) showed that nonlinear Fermi acceleration can accurately model the radio spectra of young SNRs but only when nonlinear effects from efficient acceleration are included. In fact, the standard test-particle theory of Fermi acceleration which is commonly invoked to explain the acceleration of these electrons is not consistent with the observation (Reynolds and Ellison 1993), and only when nonlinear shock smoothing (from the protons which are presumed to be present) is included do the electron spectra match the observations. These spectra actually are not power laws but show an upward curvature which may be observable with improved observations.

Further discussion of the electron acceleration problem is given in Sec. 7 below.

5. COSMIC RAYS AND ACCELERATION TO HIGH ENERGIES

(Sections 5.1–5.4 by Wefel; Sections 5.5–5.8 by Völk, except the paragraph on Völk's work in Section 5.7 by Reynolds)

5.1 Introduction

The Galactic Cosmic Rays (GCRs), those ubiquitous high-energy particles from beyond our solar system, still present an enormous challenge to theoreticians and experimentalists alike. After three-quarters of a century of investigation (dating from the pioneering balloon flights of Victor Hess ~1911–12), a full model of the GCR phenomenon is still elusive. However, the properties of GCRs, i.e., chemical composition, intensity, energy spectra, anisotropy, and temporal variation, are now reasonably well understood. What remains is to develop a fully self-consistent model: from the source(s), through injection, acceleration, propagation in the galaxy, and transport in the heliosphere, to observations at Earth.

The GCRs are a major component of modern astrophysics, intimately connected to radio astronomy and to high-energy gamma-ray astronomy as well as to galactic dynamics. It is the cosmic-ray electrons that produce the nonthermal synchrotron emission from our own and other galaxies, and the interactions of protons and electrons are the source of high-energy gamma-ray emission. Thus, the GCR problem is of importance to other branches of astrophysics and benefits from the observations made at other wavelengths.

Since the earliest days of cosmic-ray research, these connections have been emphasized (e.g., Ginzburg and Syrovatskii 1964) and, moreover, an association of GCRs with Supernovae (SN) has been postulated. There are three main reasons for a GCR–SN linkage: energy, acceleration, and composition. Maintaining the energy density of the cosmic rays in the galaxy requires a supply of energy that is easily available from supernovae. Particle acceleration occurs in SNRs as evidenced by the observed synchrotron emission, and supernova ejecta are rich in heavy elements, which may help to explain the composition of the GCRs (e.g., Wefel 1981; Simpson 1983). With the advent of first-order Fermi acceleration operating in a shock wave environment (that is, shock acceleration), SNRs become the obvious choice as sites for GCR acceleration. In fact, electrons, at least, are accelerated, since we see their synchrotron emission. The questions remain: Are protons and heavy nuclei also accelerated, and do these accelerated particles escape to become part of the GCRs?

Perhaps the most enduring prediction of shock acceleration theory is that the accelerated particles follow a power-law spectrum in momentum or rigidity. The major characteristic of the GCR energy spectrum is its power-law form extending from ~GeV nucleon^{-1} to ~TeV nucleon^{-1} energies without any apparent break or discontinuity. Below GeV nucleon^{-1} energies, the observed spectrum is modified by solar modulation during particle transport into the heliosphere. At higher energy, there is a break in the all-particle spectrum, called the "knee," at an energy between 10^{15}–10^{16} eV as shown by air-shower measurements. The origin of this "knee" is still the subject of debate, as was clear from the workshop discussions.

A prediction of shock acceleration theory, at least in the test-particle formalism, is that there is a maximum energy for the accelerated particles. This is observed directly in the spectrum of particles accelerated at heliospheric shocks as measured by spacecraft instruments (e.g., Jones and Ellison 1991). In the case of SNR shock acceleration, the maximum total energy of an ion of charge Z has been estimated to be $\sim 10^{14}\ Z$ eV in the quasiparallel geometry (e.g., Lagage and Cesarsky 1983). Such a prediction is not uniformly accepted, with Jokipii, for example, showing that for quasiperpendicular shock geometries, the upper energy limit could be much larger. *Völk* argued that, in either case, the models using the test-particle approach were too simple. In realistic environments one must consider the combined system of thermal and nonthermal (GCR) particles and their mutual interactions. He suggested a hydrodynamic approximation as one approach and described results from a two-fluid (gas and cosmic rays) model with an assumed model spectrum. These results are summarized in Sec. 5.7 below.

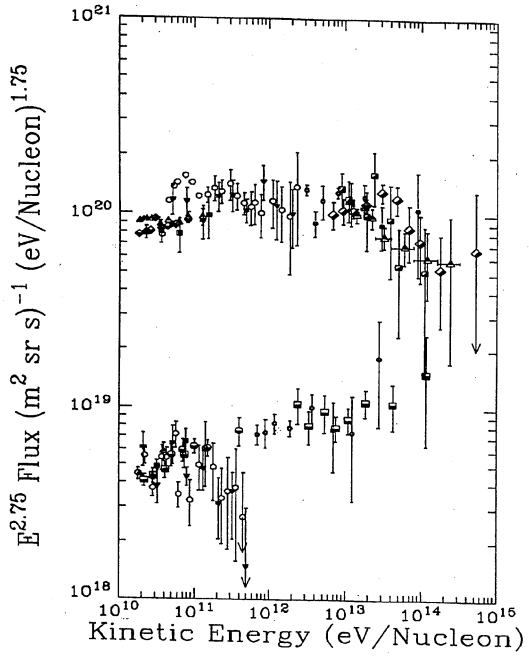

FIG. 1—Compilation of measurements of the hydrogen (top) and helium (bottom) energy spectra from 10^{10}–10^{15} eV nucleon^{-1}. Note: the vertical scale is $E^{2.75}\times$Flux.

5.2 Cosmic-Ray Observations

Experimentally, the prediction of an upper limit at $\sim 10^{14}$ Z eV does provide a signature amenable to investigation and, in either case, significant new information on the SNR acceleration process will be obtained. *Wefel* reviewed the direct measurements of individual species at high energy, based primarily on the data presented at the International Cosmic Ray Conference in Calgary, July 1993 (for a complete review see Swordy 1993). Figure 1 summarizes the high energy H and He spectral measurements, plotted as $E^{2.75}\times$ Flux versus Kinetic Energy in order to encompass many decades in flux and energy. (A spectrum proportional to $E^{-2.75}$ would be a

horizontal line on such a plot.) Between 10^{11} and $\sim 5\times10^{13}$ eV nucleon^{-1}, the protons (top) do follow a horizontal line reasonably well. The helium nuclei (bottom), however, show a different spectrum over the same energy range. The power-law spectral index for H is $\sim$2.75 while for He it is $\sim$2.65. Thus, at the highest energies, hydrogen and helium appear not to follow the same power-law spectrum. This may be interpreted as the result of nonlinear effects which must be included in the shock acceleration formalism as proposed by Ellison (1993), or as evidence for two different acceleration sites, i.e, two separate types of SNR, as discussed by Biermann (1993) (see Sec. 5.6 below). In the latter case, Biermann showed that the wind-type SNRs, as opposed to the bare SNRs, could yield just such a difference in the spectral indices.

At energies above $\sim 5\times10^{13}$ eV nucleon^{-1} in Fig. 1, there is an indication that the proton spectrum begins to steepen. The statistical weight of the different measurements is still quite small, but there seems to be a trend towards lower flux values. If this is interpreted as the maximum total energy for the acceleration, then it would be expected that the helium should show similar effects at a kinetic energy $\sim Z/A$ times the proton break point energy, i.e., at ~ 2–3×10^{13} eV nucleon^{-1}. No such steepening is observed for the helium, again within the meager statistics. This could imply that (1) the theoretical prediction of a maximum total energy $\sim Z\times E$/proton is oversimplified, (2) the protons and helium actually do come from separate SNR accelerators, each having a different maximum energy, or (3) the cosmic-ray data are still not reliable enough for such an interpretation.

Nanjo presented details of an experimental technique using emulsion chambers and a newly developed screen-type X-ray film that allows detailed study of $Z>6$ nuclei with good charge resolution and high statistics at energies up to $\sim$TeV nucleon^{-1}. He showed that secondary-to-primary ratios in the region around iron continue to decrease with increasing energy in accord with results on the B/C secondary-to-primary ratio reported by the CRN experiment (Swordy et al. 1990). He also reported a spectrum for silicon that is considerably steeper than the spectra of neighboring elements, as was also seen by Grunsfeld et al. (1988). *Shibata* combined the data reported by Nanjo with previous observations and analyzed the results in terms of a simple leaky-box model for cosmic-ray propagation in the Galaxy (for a review of the leaky-box model see, e.g., Ormes and Freier 1978). He showed that for reasonable propagation parameters, the data could be fit with a single set of assumptions about the GCR source abundances and energy spectra, again with the exception of silicon. Using these results to construct an all-particle spectrum, Shibata suggested that the "knee" may not be as sharp a spectral feature as has been inferred from the air-shower measurements.

Webber reviewed the GCR composition data from the lowest to highest energies. With the possible exception of the proton and helium spectra at high energies and the silicon anomaly mentioned above, it is remarkable that the spectra of the heavy primary elements, He, C, O, Mg $\cdots$ Fe, all are the same below 100 GeV nucleon^{-1} and appear to be the same at higher energies as well (see also Swordy 1993). This suggests that the acceleration site for helium and the heavier nuclei is the same, with only the protons requiring, possibly, a separate acceleration. (Of course, the softer silicon spectrum, if confirmed, runs counter to this conjecture.)

5.3 Long-Duration Ballooning

The cosmic-ray energy spectrum measurements are beginning to provide new constraints on the potential acceleration mechanisms in the SNR environment. One thing is clear. There is a considerable amount of work, both theoretical and experimental, that is still needed before we can fully understand, and model, the GCR acceleration process. The high-energy regime holds, perhaps, the greatest promise for new information, and *V. Jones* described a new initiative that is being considered by NASA. The GOAL (Galactic Origin and Acceleration Limit) initiative would extend the existing measurements (cf. Figure 1) by another order of magnitude in energy, allowing the possible falloff in the proton spectrum to be studied in detail and providing greatly improved spectral measurements for all of the elements through iron. Spectral differences, if they exist, including the silicon problem, could be resolved. The technique is to use the emerging Long Duration Ballooning (LDB) capability to achieve an order of magnitude larger exposure per flight and to have an intensive campaign of 2–3 flights per year devoted exclusively to gathering the new data. Combined with a program of theory/modeling of the acceleration process in realistic environments, the GOAL project would be able to provide some answers in $\sim$5–7 yr after initiation and funding.

The LDB capability is the key to the GOAL program since expensive shuttle or satellite flights would not be needed. Existing technology, both passive emulsion chambers and electronic transition radiation counter systems, can be used. The passive and active systems complement each other and also overlap to cross check the experimental results. LDB flights of over 200 hr have already been demonstrated and even longer fights are possible from the polar regions. Thus, a "quantum step" forward in both the quantity and quality of the ultrahigh-energy GCR data is now possible experimentally.

5.4 Composition Questions and Gamma-Ray Emission

The GCR energy spectra, however, are not the only constraints on the SNR acceleration model. Webber reviewed the relative composition of the GCR particles and emphasized that the composition, at the source(s), is not simply Interstellar Medium (ISM) or supernova ejecta material. Differences with the ISM include a C/O ratio of unity, the large abundance of the isotope ^{22}Ne, the underabundance of nitrogen, and the low concentration of H and He in the GCRs. The correlation of the ratio of the GCR source abundance to the ISM abundance with the first ionization potential of the elements (e.g., Wefel 1991; Ferrando 1993) brings up the injection problem. Quasiparallel shocks have been observed to accelerate thermal particles in the heliosphere and plasma simulations of quasiparallel shocks clearly show injection occurring (e.g., Ellison et al. 1990). Any ions which are pre-energized before encountering the shock will be enhanced in

the acceleration process. However, the question remains as to how the apparent first ionization potential selection is introduced: Are the thermal ions already preselected, or is there a pre-energization which produces the selection, or are the compositional biases intrinsic to the acceleration process itself (e.g., Ellison 1990)? These effects remain as major unanswered questions for the SNR model. It would appear that the material to be accelerated cannot be only supernova ejecta, which does have a large flow velocity and turbulent motions, but must involve also swept-up circumstellar or ISM material. Perhaps high-resolution spectroscopic studies of SNRs which are now becoming available will shed new light on this long-standing problem.

Another area of investigation mentioned by Völk, Webber, and others is the expected gamma-ray emission from SNRs. The gamma-ray luminosity is expected to increase with time as the SNR evolves, but the exact nature of the emissivity is still uncertain since it depends on the injection history and on any modification to the local ISM by the progenitor star. Perhaps detailed observations of gamma rays from SNRs in the coming years will be able to constrain the parameters, which will then yield corresponding information on the acceleration process for the GCR.

5.5 Maximum Energy in Fermi Shock Acceleration

The theoretical appeal (and perhaps also the success, if there is one) of diffusive particle acceleration in quasiparallel plasma shocks comes from its apparent robustness: ions with suprathermal energies can enter a Fermi process of scattering in hydromagnetic (MHD) wave fields in the quasisteady compressional flow of the shock. Although most scatterings occur either within the upstream or the downstream region of the shock discontinuity, and do not change the particle energy, the few scatterings across the shock discontinuity give to an exponentially decreasing number of particles a momentum that increases exponentially with time. This results in a simple power-law distribution in momentum. The accelerated particles at the shock diffuse ahead into the upstream plasma, self-consistently exciting their own scattering MHD waves in a resonant plasma instability. The relative magnetic fluctuation amplitude $\delta B/B$ is orders of magnitude larger than in the ambient interstellar medium (ISM) and approaches unity for very strong shocks. The nonlinear modification of the shock discontinuity enhances—and does not quench—the overall energy density of the accelerated, nonthermal particle component. (For recent reviews see, e.g., Blandford and Eichler 1987; Berezhko and Krymsky 1988; Jones and Ellison 1991).

No fine tuning of any sort is required for such a system over a wide range of parameters of the unperturbed upstream medium. The obvious limitation of this mechanism is given by the fact that the mean free path $\lambda(p)$ for pitch-angle scattering cannot become smaller than the gyroradius $r_g(p)=cp/(ZeB)$ (i.e., the Bohm limit), where p, Ze, and B denote particle momentum, charge, and average magnetic-field strength, respectively. If particle speed is denoted by βc, then the acceleration time $\tau_{acc}\equiv p/(dp/dt) = O[\lambda(p)\beta c/U_1^2]$ at a shock speed U_1 has a lower bound for a given p. Integrating this equation for dp/dt over the finite lifetime of any real system, like that of a SNR, gives an upper limit p_{max} (Bohm). For a typical SNR in a uniform medium this gives 10^{14} to 10^{15} eV/c^{-1} for protons, barely reaching the knee of the observed Galactic Cosmic Ray (CR) distribution at an energy $\simeq 5\times10^{15}$ eV (see Fig. 1). Skeptics believe that p_{max} (Bohm)$\leq 10^{14}$ eV/c^{-1} (e.g., Lagage and Cesarsky 1983) due to the nonuniformity of the upstream wave field.

Thus SNR acceleration may not only fail to give the CR spectrum above the "knee" spectral break, requiring some unknown (re)acceleration effect beyond, but may not even reach the knee. In this situation *Jokipii* (1987) examined the acceleration possibilities at perpendicular shocks, where the shock normal is perpendicular ($\perp$) to the direction of the average upstream magnetic field $\langle\mathbf{B}\rangle$. Jokipii reviewed and reemphasized his conclusions at the workshop. He first argued that the diffusion coefficient $\kappa_\perp(p)$ for transport perpendicular to $\langle\mathbf{B}\rangle$ can be considerably smaller than $(1/3)\beta c r_g(p)$ if the parallel ($\parallel$) mean free path $\lambda_\parallel(p)\gg r_g$, although he requires $\lambda_\parallel/r_g \leq \beta c/U_1$ for diffusion across the field to be efficient. A SNR in the uniform field of a uniform ISM has large portions of its surface parallel to $\langle\mathbf{B}\rangle$; numerical models indicate that $p_{max}\simeq 10^{16}$ eV/c^{-1} for protons could be reached. Acceleration can be viewed as energy gains of particles drifting across $\langle\mathbf{B}\rangle$ in the $\mathbf{u}\times\mathbf{B}$ electric field of the shock frame of reference. Jokipii concluded that the so-called "Bohm limit" is *irrelevant* to diffusive shock acceleration.

This last statement generated some discussion in Raleigh. The first question concerns particle injection. While for thermal electrons, the mobility along $\langle\mathbf{B}\rangle$ may be high enough so that they can be sufficiently energized in the upstream lower hybrid turbulence excited by thermal ion reflection at the shock front (Galeev et al. 1993), there is no easy way for thermal ions from the shocked downstream plasma to escape upstream along $\langle\mathbf{B}\rangle$ and to participate in spatial diffusion across the shock as in a quasiparallel shock. How does one inject ions here? The other question regards the robustness, i.e., the wave field necessary to produce a $\lambda_\parallel/r_g$ of the right magnitude. The resonant CR instability does not exist for strictly perpendicular shocks. How is the wave field provided for the Fermi process to operate? In a uniform ISM, upstream waves convected into the shock would have to exist for the entire SNR lifetime at the right magnitude to produce the highest-energy particles towards the end of the SNR evolution. Unless a new wave excitation process can be invoked, the pre-existing scattering properties of the ISM alone do not appear to provide this scattering by a large margin: for an average ISM diffusion coefficient $\kappa\simeq 10^{29}$ cm^2 s^{-1}, from Galactic escape arguments for a 10^{10} eV proton, and $B=3\times10^{-6}$ G, $\lambda_\parallel/r_g\simeq 10^6$. From the above statistical mechanics argument in turn this ratio has to be smaller than $\beta c/U_1$, at such energies. This would require $U_1\simeq 0.3$ km s^{-1}, generally much smaller than ISM sound speeds. Therefore, on average at least, ISM scattering is too weak. Perhaps shock-induced drift instabilities might exist which can propagate into the upstream precursor region of the shock. Present models (Pajot-el-Abed et al. 1992) are probably not adequate for this purpose. It would be very nice if a

robust mechanism could also be found for such perpendicular acceleration over long time scales. (See Sec. 4.4 for a discussion of simulation results on oblique shocks.)

5.6 Highest-Energy Cosmic Rays

Biermann used a different approach to achieve the CR energy spectrum above $p \simeq 10^{14}$ eV/c^{-1} in SNRs. He radically extends the simple-minded argument (Völk and Biermann 1988) that SN explosions into the wind flow of a very massive progenitor star could result in rather high maximum proton momenta of the order of 10^{15}–10^{16} eV c^{-1} because the circumstellar magnetic field $\langle \mathbf{B} \rangle$ can be very strong (making r_g and τ_{acc} small). He argues that at least very young (during sweep-up?) shell-type SNRs [of age $<10^3$ yr, as Dickel reiterated (see Sec. 3.1), confirming his earlier findings] have largely a radial structure in their magnetic fields near their boundary (Dickel et al. 1991), although nominally $\langle \mathbf{B} \rangle$ should be more tangentially oriented. Biermann concludes that this indicates rapid turbulent plasma convection in directions perpendicular to the shock front. At least in the downstream region, inside the SNR, this is understandable due to subsonic flow inhomogeneities, arising in the SN ejecta, or being induced by interstellar clouds swept over by the shock. On the other hand, it is hard to see why these arguments should imply similar turbulent convection upstream of the shock. Then Biermann uses Prandtl's mixing length arguments (Prandtl 1925) for ordinary fluid dynamics, and constructs a turbulent energetic-particle diffusion coefficient from the macroscopic fluid scale l, assumed to equal 1/4 of the shock radius r, and the characteristic velocity difference $U_1 - U_2$ across the shock. Thus he postulates a downstream (subscript 2) radial diffusion coefficient $\kappa_{rr,2} = (U_2/3U_1) r (U_1 - U_2)$, independent of energy (diffusion by turbulent convection). Apart from the factor $U_2/U_1 (= 1/4$ for strong shocks) the same diffusion coefficient is also used upstream of the shock. These postulates are the big steps. Then $r_g(p_{max}) = r$ is used to obtain $cp_{max} = ZerB_1$, whereas one might argue that $\kappa_{rr} = (1/3)\lambda(p)\beta c \geq r_g(p)\beta c/3$, since r_g is the smallest convection scale for a particle of momentum p. This results in $cp_{max} = [(U_1 - U_2)/\beta c] \cdot ZerB_1$, which is at least a factor of order 10 smaller than $ZerB_1$. By considering the geometry of the wind magnetic field and the resulting particle drift effects, Bierman also derives an energy beyond which acceleration is less rapid, identifying this energy with the knee in the spectrum. For surface fields of Wolf–Rayet stars of the order of a few thousand Gauss (cf. Maheswaran and Casinelli 1992), and taking $rB \simeq 3 \times 10^{14}$ G cm≈const, he obtains $cp_{max} = 9 \times 10^{16}$ eV for protons and $cp_{max} = 3 \times 10^{18}$ eV for iron nuclei ($Z = 26$).

Thus, at least at the highest energies attainable in such a manner, the chemical composition should be dominated by heavy ions. Indeed, as long as the SNR shock runs through previous wind material, say of a Wolf–Rayet star, the chemical and isotopic composition should reflect the wind composition together with the rigidity cutoffs.

In this context, it is perhaps important to mention that the total, time-integrated mass in the progenitor wind is of the same order as the supernova ejected mass. Thus the magnetic-field topology of a stellar wind exists for the SNR mostly during the SNR sweep-up phase. As a consequence, most of the gas heating (and production of the bulk of the energy in CRs) in a SNR occurs in the ambient ISM, partly swept up by the progenitor wind and turbulently mixed (e.g., Kahn and Breitschwerdt 1989) with hot wind gas from beyond the wind termination shock. During this later phase the SNR shock is probably well described again by a quasiparallel shock, with the relevant $\langle \mathbf{B} \rangle$ directions given by those of the turbulent eddies that correspond to the diffusion length of the energetic particles considered.

Biermann argued that the observations are consistent with the derived spectra and composition, and that (independently) he has a persuasive source model for the observed ultrahigh energy CR particles ($cp >$ few 10^{18} eV) to be produced in the hot spots of radio galaxies (Rachen and Biermann 1992). However, substantial discussion took place on some of his basic postulates. In writing, others have considered the dynamic effects of the large stellar magnetic fields invoked in this phenomenological theory (Axford 1991).

5.7 Two-Fluid Model of Fermi Acceleration

In contrast to the presentations of Jokipii and Biermann who were largely concerned with perpendicular shocks and concrete astrophysical acceleration scenarios, *Jun* (jointly with Norman) considered nonlinear aspects of the theory without direct astrophysical application. Concretely he investigated the dynamical effects of $\langle \mathbf{B} \rangle$ in the evolution of plane CR-mediated shocks. Based on a two-fluid model he first treated steady-state solutions. While this can be done analytically, the time-dependent system of a piston-driven nonlinear CR shock requires a carefully devised quasiexplicit numerical scheme. The results concern the transient behavior of the shock (which depends on the size of the effective diffusion coefficient) as well as the approach to an asymptotic steady state. For strong shocks, the strong early gas heating gives way with time to a dominant CR energy production in (partially) modified shocks. Finite $\langle \mathbf{B} \rangle$ implies smaller acceleration efficiency and weaker shock modification at given Mach number. So this work confirms and extends known results obtained by others. Jun announced the intent of his group to discuss the instability of the shock precursor (Dorfi and Drury 1985) with this technique in the oblique case. This would be a very valuable contribution to the theory of nonlinear CR shocks, both theoretically, and in particular observationally, as far as the temperature structure of the gas is concerned.

Völk described work elaborating the two-fluid description of particle acceleration in which two sets of coupled fluid equations are used to describe a thermal-gas fluid with adiabatic index $\gamma_G = 5/3$ interacting with a cosmic-ray fluid with γ_c between 4/3 and 5/3, depending on the cosmic-ray distribution function. This method has been used to calculate cosmic-ray spectra accelerated in evolving SNR shocks as well as in other situations such as galactic winds and AGN. It has virtues of relative computational efficiency, and the possibility of describing large-scale hydrodynamics of compli-

cated systems. Since cosmic rays are probably accelerated with substantial efficiencies in SNRs, their dynamical contributions must be included there, and probably elsewhere when strong shocks are present. However, the method has several drawbacks. Particle injection is normally treated by fixing a proportion of particle flux or shock energy entering the cosmic-ray population, so that self-regulation is not possible, allowing nonphysical effects in steady-state solutions. Also, two important parameters whose values depend on the detailed cosmic-ray distribution function cannot be calculated self-consistently but must be specified: the cosmic-ray index γ_c, and the mean diffusion coefficient κ (averaged over the cosmic-ray distribution). Völk devoted his presentation to an attempt to improve the description of those two parameters in the context of the two-fluid method.

This was done by essentially guessing an approximate form of the cosmic-ray distribution function in terms of parameters whose values can be calculated in the two-fluid context. If an acceptable analytic approximation for the distribution function $f(p)$ were known, γ_c could be calculated directly, and κ could be formed given a physical model for the actual momentum-dependent coefficient $\kappa(p)$. Two such model distribution functions were described, a broken power-law description and a single power-law plus delta-function "bump." The quality of these approximations varies during the evolution of a SNR; for "intermediate times" such that particles will have been accelerated to of order 100 times their injection momentum (assumed constant), the "bump" description is better, while the broken power-law is fairly reasonable at late times. These approximations were tested against a more detailed calculation involving solving the transport equation for the cosmic-ray population numerically, simultaneously with a set of hydrodynamic equations for the thermal gas (Berezhko et al. 1993). Fairly reasonable agreement was obtained, with an additional adjustable parameter fit by comparison with the Berezhko calculation. Völk concluded that the model could provide a good description of the more detailed calculation, and that the chief problems were not the cosmic-ray transport or nonlinear dynamics, but the physics of injection, still fundamentally untreatable in this picture.

5.8 Particle Diffusion in Random Fields

Ptuskin reminded the workshop that particle diffusion in random fields has many more aspects than just pitch-angle diffusion. This is simply due to the fact that chaotic motions of an ionized gas into which the magnetic field is frozen lead to chaotic field structures. Energetic particles, even if they are strongly magnetized ($r_g \ll \lambda$), sample these field structures in their motion along field lines, and apparently diffuse across the large-scale mean field. Ptuskin contrasted the concepts of field-line random walk and compound diffusion with a new formula for the effective diffusion coefficient $\kappa_\perp$, perpendicular to the direction of the large-scale field. Besides local parallel diffusion, it contains local perpendicular and Hall diffusion, turbulent diffusion, and nonstatic wandering of field lines (taking into account the finiteness of the Alfvén velocity), as well as the stochastic divergence of close field lines. Even if the principal scale L of the MHD turbulence fulfills the inequality $r_g \ll \lambda \ll L$, together with $\langle(\delta B/B)^2\rangle \ll 1$, the turbulence cannot be considered weak any more, if $\langle(\delta B/B)^2\rangle$ exceeds r_g/λ. This has important consequences for CR diffusion across the disk of the galaxy since the mean field $\langle \mathbf{B} \rangle$ there is quite strongly azimuthally directed, with only a very small component perpendicular to the disk.

These effects may also play a role in acceleration in perpendicular shocks. Probably a strictly perpendicular field exists only in local regions and for short times. This may make particle injection a rather intermittent process. However, for the higher-energy particles the diffusion times are large enough to smear out such time variations quite readily. The large parallel diffusion coefficients in the ISM sufficiently far ahead of the shock (as inferred from Galactic escape time considerations) will assist particles to return to the shock at another point somewhat later, even if they were locally convected across the shock discontinuity on a locally perpendicular field line (i.e., a field line parallel to the shock surface). This should also allow the development of the upstream resonant instability as in the quasiparallel case. Whether such a situation leads to such high maximum momenta as argued by Jokipii (Section 5.5) on a quite different basis, is quite another matter to be investigated. However in a statistical sense the process should have a similar robustness as quasiparallel shock acceleration, eliminating the need, at least in the ISM, to consider truly perpendicular shocks.

6. SHOCK PRECURSORS AND OPTICAL OBSERVATIONS

6.1 Introduction

Models for the diffusive shock acceleration of cosmic rays require that particles scatter back and forth between the shock jump and an upstream region of plasma turbulence if they are to reach high energies. The extent of this upstream region, i.e., the shock precursor, depends on the acceleration efficiency and the diffusion length of the energetic particles.

There are several aspects of this acceleration mechanism that have potentially observable consequences:

(1) The densities of cosmic-ray nuclei and electrons behind the shock will be greater than can be provided by the van der Laan mechanism (1962) of simple compression and betatron acceleration (i.e., adiabatic heating).
(2) This enhanced density of nonthermal particles should extend outward beyond the shock jump (the gas subshock).
(3) There should be enhanced turbulence in the immediate preshock medium.
(4) Cosmic-ray pressure on the scattering wave turbulence should be transferred to the ambient ion gas, causing acceleration of the preshock medium to some fraction of the shock velocity, and a corresponding compression.
(5) Damping of the wave turbulence should cause heating of the preshock medium. Predicted values for the associated observables are too seldom presented in theoretical papers, but they clearly depend mainly on the energy density of the nonthermal particles and on the cosmic-ray diffusion coefficient, the latter setting the scale of the

precursor. A pioneering attempt to connect the acceleration theory to observations of a real SNR was made by Boulares and Cox (1988).

The speakers in this session discussed the present status of attempts to confront these expectations with observations of supernova remnants. The bottom line is that there is presently no convincing evidence that real supernova remnants have cosmic-ray precursors ahead of their shock fronts.

6.2 Synchrotron Precursor

Reynolds discussed the expected structure of the precursor as seen in synchrotron radiation. His conclusion was that any precursor must be very thin not to have been detected thus far. Within the diffusive acceleration model this requires a much higher level turbulence than is present in the general ISM, favoring the dominant view that the cosmic rays themselves generate the turbulence. Inferred levels of $\delta B/B$ are an order of magnitude or much greater than ISM averages, i.e., $\delta B/B \gtrsim 0.01$ versus $\delta B/B \sim 0.001$ for the ISM. The present observational status is that no synchrotron precursor has yet been seen, though if they exist, they should be found with conceivable advances in observational technology. The alternative is that nonthermal electron confinement to the postshock region takes place via some other unspecified (nondiffusive) mechanism.

Spangler discussed attempts to detect effects of turbulence in the precursor as modifications to the characteristics of background radio sources. The conceivable effects include angular broadening, intensity scintillations, pulse broadening, and spectral corrugation. Several radio sources close to SNRs, but beyond their apparent boundaries, showed no evidence for angular broadening beyond the typical interstellar values. The radio source CL 4 behind the Cygnus Loop, however, did show strong broadening though it is unclear where the responsible turbulence is located. It could be in a precursor, but it could just as well be behind the shock where amplified turbulence of the general ISM is expected. It could be even deeper within the remnant as unrelated fluctuations. What we know for certain is that there is appreciable turbulence somewhere within at least one remnant, turbulence that could be related to a precursor, but any precursor must be thinner than the projected distances between the radio sources and the SNR limbs studied thus far. The latter is fully consistent with the other limits on the precursor thickness from Hα, synchrotron, X rays, etc.

6.3 Cygnus Loop

Hester and Shull discussed the spatial complexity of the Cygnus Loop. Hester's *HST* images showed the importance of small-scale inhomogeneities and shear instabilities in creating the observed morphology, as well as the importance of variations of the transverse component of the magnetic field in limiting shock compression. If turbulence and shear are important for accelerating particles and amplifying magnetic field, then 1-D diffusive acceleration models maybe very difficult to compare with observed SNRs. Shull discussed evidence that the Cygnus Loop is an encounter between a supernova blast wave and a dense shell open on one side, created by the precursor. If—as Shull, Hester, and other past students of the Loop have suggested—the Cygnus Loop is in a very brief evolutionary phase while the blast wave overtakes a dense shell, one must be careful in using it to infer average SNR characteristics for use in global estimates of CR acceleration.

6.4 Hα Line Profile

Smith (for collaborators Blair and Raymond) discussed connections which are expected to exist between the Hα profile of Balmer-dominated shocks and the cosmic-ray precursor. The interrelation should provide a very useful test of the existence and properties of precursors, sampled on an extremely small scale.

There is a straightforward model for the line profile in a Balmer-dominated shock, without postulating a cosmic-ray precursor. It requires fast (nonradiative) shocks entering partially neutral gas. The Balmer line emission arises from neutrals which are excited to radiate before being collisionally ionized, roughly one atom in five producing an Hα photon. Because the neutrals do not feel the turbulence or the electromagnetic fields of the collisionless shock, they can be excited while they still have their preshock velocity distribution, producing a narrow Hα profile. Some atoms undergo charge transfer before excitation, however, producing a subpopulation of neutrals with the velocity profile of the postshock ions, contributing a broad base to the line.

The above model has been used successfully to interpret Balmer-dominated shock emission over a wide range of shock velocities and remnant evolutionary stages (e.g., Smith et al. 1994, and references therein). It appears to have only one major flaw: the narrow part of the line profile is much too wide to be representative of the ambient preshock temperature. As a result, there has been a significant flurry of hopeful activity attached to the possibility that the additional linewidth might be caused by the cosmic-ray precursor.

In this case, the bottom line is that there is no clear way to solve the problems of the Hα profile with a cosmic-ray precursor. The profile remains a mystery and the precursor appears not to exist. (Note that the latter statement is much more forceful than one saying that the precursor has not yet been found. It did not appear in our earlier bottom line only because the results are still tentative.)

It was expected that the additional width in the narrow Hα component could be due either to the preshock heating of the ambient gas in the precursor, or to the presence of preshock turbulence. In either case it was necessary to transfer the velocities to the neutrals via collisions (primarily charge exchange). In addition, the observed linewidths of 30 to 50 km s^{-1} correspond to temperatures of 20,000 to 50,000 K. If the electrons had this same temperature, the neutrals would soon be ionized in the precursor. One requires that the heating be very sudden, to avoid ionization, or that the neutral velocities not be indicative of the electron temperature. If the electrons are hot, the diffusion coefficient must lie in the range 10^{23} to 10^{24} cm^2 s^{-1} so that the neutrals flow too quickly through to get ionized. Wave dissipation, however,

may not lead to equal electron and ion temperatures. The electrons, being capable of collisional losses, may remain cool even in the presence of hot ions. In addition, if dissipation occurs via neutral ion drag, it may directly heat the ions and neutrals. Although there are uncertainties, one gets the impression that a viable model may be possible. One constraint is that it must produce similar narrow component widths for a tremendous range in shock velocity.

The reason that the second bottom line was so pessimistic is that a potentially major problem surfaced at the meeting. According to theory, the precursor should accelerate the preshock medium to a significant fraction of the shock velocity, but the narrow Hα component from the LMC SNRs 0509-67.5 and 0519.69.0 do not show any evidence for the expected velocity shifts. It is very important that further observations be made to generalize one and quantify these results. If they stand, there is no appreciable precursor, at least in these shocks entering partly neutral gas.

Consistent with the above result, it was the consensus of several of the participants that very often the van der Laan mechanism is sufficient to provide the observed radio synchrotron. An interesting and related recent preprint by Naito and Takahara (1994) finds that the high-energy gamma-ray emission from the nuclei accelerated by SNRs should be detectable against the background. It should prove very interesting to see whether they are really there.

7. COSMIC-RAY ELECTRONS AND PROPAGATION

7.1 Introduction

The problem of the shock acceleration of electrons has been a major concern of shock acceleration theory for some time. While electrons provide our only *in situ* probes of shock acceleration outside the heliosphere, their injection has not been understood nearly as well as that of protons. Not only has an injection mechanism been missing, whereby thermal electrons might be picked up and accelerated, but even rough ideas of the global efficiency with which electrons are accelerated have not been available, let alone the possible evolution of that efficiency with shock strength, shock obliquity, or other parameters. On the observational side, however, supernova remnants in our Galaxy and other galaxies offer substantial assistance in investigating this problem, through the investigation of radio synchrotron emission. *Levinson* offered new theoretical ideas which may lead to a better understanding of the mechanism of electron injection, while *Rudnick* presented detailed observations of Cassiopeiae A and *Duric* described a global study of supernova remnants in M33 and of the overall cosmic-ray electron population in M33.

7.2 Analytic Model for Electron Injection

Levinson summarized the difficulties of injection of electrons: thermal electrons see the shock as a smooth change in fluid properties, not as an abrupt discontinuity, and will merely be adiabatically heated unless there are waves present, embedded in the flow, to scatter the electrons. The most effective scattering process is resonant, i.e., scattering by waves with wavelengths comparable to the particle's gyroradius; nonresonant scattering is negligible. Thus the waves scattering electrons cannot be the Alfvén waves produced by the protons, which then scatter (inject) a few protons into the nonthermal tail of the distribution, because those waves have much too long wavelengths for resonant interaction with thermal electrons. Once electrons have $p \sim m_i v_A \sim 200$ keV, where v_A is the Alfvén speed, they may scatter from proton-generated waves, if those are present. However, since electrons with energies below ~ 1 GeV have longer upstream diffusion lengths than protons, no proton-generated waves will be present far upstream and the electrons must produce their own waves. Thus the electron injection problem is the nature of the mechanism boosting electrons to ~ 1 GeV. Levinson investigated carefully a frequently rejected possibility, whistler waves, and showed that in fact they might fill the bill very nicely, at least for strong shocks ($\mathcal{M}_A \geq 43$), though this condition may be relaxed in some situations.

Whistlers had been rejected for two reasons: first, their equilibrium energy density is small in a normal plasma, and second, electron-produced field-aligned whistlers can only scatter electrons moving in the opposite direction, so as electrons stream ahead of the shock, their on-axis whistlers cannot turn around other forward-streaming electrons. Levinson pointed out that the second difficulty is removed by considering off-axis waves, while the first is not relevant: any energy density in waves simply provides some diffusion coefficient, and if this corresponds to a long mean free path, so much the better: the acceleration process is more efficient. Levinson obtained an estimate from quasilinear theory for the diffusion coefficient from electron self-generated whistlers, which he used to calculate numerical electron spectra. He found that the diffusion coefficient rises with electron energy; also, as it rises, the injection efficiency decreases. (This is also true for protons, so that self-regulated nonlinear shocks are stable.) He also showed that the most obvious damping processes that might invalidate the quasilinear calculation of the diffusion coefficient are probably not important if $\mathcal{M}_A > 13$.

The importance of these results is considerable. Self-generated whistlers can inject thermal electrons directly into the first-order Fermi process if $\mathcal{M}_A > 43/\sqrt{\beta_e}$, where $\beta_e = n_e k T_e/(B^2/8\pi)$ which is normally of order unity upstream of a SNR shock. Thus $\mathcal{M}_A > 43$ is probably sufficient; but it may not be necessary. If electrons simply have their velocities randomized in the shock, they will have a post-shock temperature $T_{e2} = (m_e/m_i) T_{i2}$ and it may be that $\beta_{e2} \sim \beta_{e1}$. Electron–ion equilibration, if due only to Coulomb collisions, might take a very long time. However, the evidence from X-ray observations of high electron temperatures immediately behind the shock suggests that some kind of non-Coulomb process heats electrons, so that $\beta_{e2} \gg 1$. Then the condition on the shock strength is greatly relaxed. Even if the condition is not met, the injection problem will have been greatly reduced: one merely needs to promote the electrons to energies at which self-generated whistler acceleration can take over. The suggestion that collisionless electron heating might be sufficient (and perhaps necessary) for efficient shock acceleration of electrons implies strong cor-

relations between X-ray and radio morphology in young SNRs. This work was described in Levinson (1992).

The numerical simulations (Levinson 1994) assumed sufficient electron heating for injection by whistlers, which then carry the electrons to $E_i \sim (m_i^2/m_e)v_A^2$, above which energy they are scattered by the proton-generated Alfvén waves in the proton precursor and by electron-generated Alfvén waves beyond the proton precursor (as noted above, until $E_e \sim 1$ GeV, the electron precursor extends beyond the proton precursor). The calculation solves the diffusion equation for the electron distribution function in a fixed shock-velocity profile chosen to mimic that of a shock modified by upstreaming accelerating ions, so the electrons are test particles. Results for electron spectra show substantial efficiency at electron acceleration, and are relatively insensitive to shock parameters (except the smoothing length scale from proton acceleration). The electron/proton ratio also depends only weakly on shock parameters: at GeV energies, it is 1%–10%, in the range measured in the cosmic rays at energies of a few GeV. While this agreement is very heartening, it is not clear that one should expect these numbers to agree, since shock evolution and propagation effects intervene between a single strong shock and the cosmic-ray pool we sample at Earth.

7.3 VLA Observations of Cas A

Rudnick reported on extensive VLA observations of Cas A, including spectral-index studies and examinations of brightness changes and proper motions of discrete radio features. The goal of this study was to identify characteristics of regions showing enhanced synchrotron brightness, to try to understand the physical nature of particle acceleration. Rudnick summarized several related projects, from the Ph.D. research of Anderson. Both new observations with earlier observations performed by others were used to obtain this information. The spectral-index observations used extensive filtering, appropriate if bright radio knots represent discrete physical objects which can be divorced from the smoother background of radio emission on which they sit. (If this assumption is not correct, the filtering can produce misleading results.) A large dispersion in spectral index of these features was found: $\alpha \sim -0.5$ to -0.9 ($S_\nu \propto \nu^\alpha$), where the remnant mean is about -0.77. Brightness changes of up to 20% per year were observed in individual features, both brightening and fading. Finally, proper-motion studies showed substantial variation in different quadrants around the remnant, expansion time scales R/v varying by a factor of 3, between 500 and 1700 yr. (Since the age of Cas A is presumably about 320 yr, all radio knots are decelerating.) The systematic variation of these rates suggests that the motion of knots cannot be decomposed into a uniform expansion with superposed random motions, but that coherent variations in the extent of deceleration are taking place.

Correlations of knot properties then showed that neither knot brightness, the sign of brightness change, or expansion time scale was correlated with knot spectral index. However, a strong correlation between knot radius and spectral index was found: knots closer to the center had systematically flatter spectral indices, leading to the inference that only the position, not the physical state of a knot, determined its spectral index. Furthermore, a correlation was observed between rate of brightness change and position: beyond the peak of the radio ring, the rate of brightness change increases with distance. These results were compared semiquantitatively with two-fluid simulations of Jones, Kang, and Tregillis (in preparation) of ejecta clumps decelerating in a SNR expansion. Rudnick concluded that turbulent amplification of magnetic fields, like that appearing in the simulations, is the chief cause of brightness increase of synchrotron knots, and that that amplification is powered by knot deceleration. The poor correlation index with most properties suggested to Rudnick that the currently bright features are not the sites of electron acceleration. Apparently the simulations did not include the possibility of second-order turbulent (stochastic) acceleration, which would also be deceleration powered. The wide range of knot spectral indices would, in a shock-acceleration picture, require an enormous range of shock Mach numbers $\mathcal{M}$, explainable only as clump bow shocks into already shocked material, providing $\mathcal{M} < 5$ or so required for significant changes in spectral index from the $\mathcal{M} \to \infty$ asymptotic value ($\alpha = -0.5$).

7.4 Cosmic Ray Electrons in M33

Duric summarized radio studies of M33 with Westerbork and the VLA, addressing the question: could the observed SNRs in M33 account for the overall diffuse emission due to cosmic-ray electrons in M33? About 48 SNRs were identified; they had spectral indices distributed about a mean of -0.5 with a dispersion of about 0.2, while the mean disk spectral index was -0.9 ± 0.1. This steepening could be reasonably described with a simple diffusion model with a diffusion coefficient depending on energy as $D(E) \propto E^{0.8}$. This spectral-index distribution is slightly flatter than in our galaxy, and the presence of substantial numbers of SNRs with spectral indices flatter than -0.5 is somewhat problematic for simple shock-acceleration theory. Energetics of SNRs were addressed using equipartition minimum-energy estimates for each. The distribution in minimum energy U was fairly symmetric in the log, with $\log \bar{U} = 49.6$ ($\bar{U} = 4 \times 10^{49}$ ergs) and a dispersion in $\log U$ of 0.3. The total minimum energy in all SNRs was 7×10^{51} ergs, while that in the disk was 2×10^{54} ergs. Their ratio could be simply the ratio of the leakage time for electrons to leave the disk to the mean lifetime of a SNR, about 300, if equipartition roughly holds (the minimum energies are close to the actual nonthermal energies). If equipartition does not hold in the SNRs, it must still be true that the total nonthermal energy per SNR is less than the explosion energy $\sim 10^{51}$ ergs, giving a lower limit of about 50 to the ratio of times. If SNRs live of order 10^5 yr, this implies a cosmic-ray residence time in the disk of M33 of order 10^7 yr, about what it is in our galaxy. Thus the hypothesis that the SNRs we observe can account for the distributed cosmic-ray electron population in M33 is consistent with the observational information.

8. SUMMARY

The study of supernova remnants is currently benefiting from a wealth of new observational and theoretical results and is in extremely good health. This workshop demonstrated that SNRs can produce energetic discussions as well as energetic particles: several issues seemed particularly important, interesting, or contentious. Much of the discussion at this workshop focused on the realization that shock models may have to include dynamical effects of cosmic rays even to provide good descriptions of thermal physics, let alone the nonthermal particles. Workers in optical and X-ray observations expressed desires for more complete theoretical calculations of these dynamical effects presented in a form which can be compared directly with observations. For instance, the observed excess width of the narrow component of Hα reported by Smith, Blair, Raymond, and collaborators might be produced by the direct interaction of the neutral atoms with the cosmic-ray precursor as the cosmic rays stream out in front of the shock and accelerate and ionize the preshock gas. It remains to be seen if this idea will work quantitatively. In fact, while precursors are an essential part of nonlinear shocks, there is at present very little firm observational evidence for their existence in SNRs. More careful work on these and other implications of particle acceleration should be done by researchers studying nonlinear shock dynamics, while observers, especially at radio wavelengths, should search diligently for synchrotron precursors.

The workshop also saw debates over the best strategies to pursue in studying the nonlinear properties of cosmic-ray-influenced shocks. The high-acceleration efficiencies which make Fermi shock acceleration an attractive mechanism necessarily imply that the process is nonlinear and, therefore, difficult to model. Supporters of the two-fluid method, an analytic technique in which cosmic rays and thermal gas are treated as separate fluids coupled through dynamical and *ad hoc* injection terms, demonstrated more sophisticated time-dependent calculations directed toward solving the so-called closure problem. This problem occurs because parameters such as the diffusion coefficient and the ratio of specific heats, which are required to solve for the distribution function, depend on the distribution function. Supporters of computer simulations, which produce the entire particle distribution function directly, argued that failure to include better injection physics made two-fluid models unreliable. However, the simulation approach makes enormous computational demands and as yet cannot address the necessary ranges of length and time scales to cover SNR blast waves as can be done with analytic methods. Both analytic modeling and computer simulations have strengths and weaknesses and the best approach in the future may well be a combination of the two.

Morphological modeling is becoming more quantitative and is beginning to make better use of the enormous detail present in typical X-ray or radio images. Codes that use a numerical hydrodynamic substrate and sophisticated spectral modeling to predict the X-ray structure of young remnants are now operating, and may be able to extract firm conclusions from *ROSAT* images. Similar codes are being prepared to predict structure in synchrotron radio emission, both total intensity and polarization, and may prove equally productive in comparisons with radio observations.

The workshop organizers feel that important issues to watch in the next few years include new observations in X rays from *ROSAT, ASCA*, and other spacecraft, and more sophisticated spectral and spatial modeling of thermal X-ray emission; developments in the theory of electron heating and acceleration in shock waves, aided perhaps by radio polarization studies of SNRs and improved cosmic-ray observations, particularly from Long-Duration Ballooning; further use of the extremely powerful diagnostic of the nonradiative optical emission from shocks; theoretical work making predictions for this optical emission from nonlinear shock models; and the further development of powerful simulation techniques, perhaps combined with analytic calculations based on the two-fluid model. There is much to do and much to learn on the physics of these strong shock waves in SNRs, but since shocks exist in many environments from the heliosphere to extragalactic radio jets, whatever is learned of shock physics in SNRs will have fruitful application in many areas of astrophysics.

REFERENCES

Axford, W. I. 1991, in Astrophysical Aspects of the Most Energetic Cosmic Rays, ed. M. Nagano and F. Takahara (Singapore, World Scientific), p. 406

Baring, M. G., Ellison, D. C., and Jones, F. C. 1993, ApJ, 409, 327

Baring, M. G., Ellison, D. C., and Jones, F. C. 1994, ApJS, 90, 547

Berezhko, E. G., and Krymsky, G. F. 1988, Usp. Fiz. Nauk., 154, 49 (English translation, Sov. Phys. Usp., 31, 27)

Berezhko, E. G., Yelshin, V. K., and Ksenofontov, L. T. 1993, Proceedings of the 23rd International Cosmic-Ray Conference, Calgary, Invited, Rapporteur and Highlight Papers (Singapore, World Scientific), 2, 354

Biermann, P. 1993, Proc. 23rd Int. Cosmic-Ray Conf., Calgary, Invited, Rapporteur and Highlight Papers (Singapore, World Scientific), p. 45

Blandford, R. D., and Eichler, D. 1987, Phys. Rep., 154, 1

Boulares, A., and Cox, D. P. 1988, ApJ, 333, 198

Decker, R. B. 1988, Space Sci. Rev., 48, 195

Dickel, J. R., van Breugel, W. J.M., and Strom. R. G. 1991, AJ, 101, 2151

Dorfi, E., and Drury, L. O'C. 1985, Proceedings of the 19th International Cosmic-Ray Conference (La Jolla), NASA Pub., 3, 121

Draine, B. T. and McKee, C. F. 1993, ARA&A, 31, 373

Drury, L. O'C, 1983, Rep. Prog. Phys., **46**, 973

Ellison, D. C. 1990, Proceedings of the 21st International Cosmic-Ray Conference (Adelaide, Univ. of Adelaide), 11, 133

Ellison, D. C. 1993, Proceedings of the 23rd International Cosmic-Ray Conference, Calgary, Invited, Rapporteur, and Highlight Papers (Singapore, World Scientific), 2, 219

Ellison, D. C., Möbius, E., and Paschmann, G. 1990, ApJ, 352, 376

Ferrando, P. 1993, Proceedings of the 23rd International Cosmic-Ray Conference, Calgary, Invited, Rapporteur and Highlight Papers (Singapore, World Scientific), p. 279

Galeev, A. A., Malkov, M. A., and Völk, H. J. 1993, submitted to J. Plasma Physics

Ginzburg, V. L., and Syrovatskii, S. I. 1964, The Origin of Cosmic Rays trans. H. S. W. Massey, ed. D. ter Haar (New York, McMillan), p. 426
Grunsfeld, J. M., L'Heureux, J., Meyer, P., Muller, D., and Swordy, S. 1988, ApJ, 327, L31
Hoshino, M., Arons, J., Gallant, Y. A., and Langdon, A. B. 1992, ApJ, 390, 454
Jokipii, J. R. 1987, ApJ, 313, 842
Jones, F. C., and Ellison, D. C. 1991, Space Sci. Rev., **58**, 259
Jones, T. W., and Kang, H. 1993, ApJ, 402, 560
Kahn, F. D., and Breitschwerdt, D. 1989, MNRAS, 242, 209
Kassim, N. E., Hertz, P., and Weiler, K. W. 1993, ApJ, 419, 733
Klein, R. I., McKee, C. F., and Collela, P. 1994, ApJ, 420, 213
Lagage, P. O. and Cesarsky, C. J. 1983, A&A, 118, 223
Levinson, A. 1992, ApJ, 401, 73
Levinson, A. 1994, ApJ, 426, 327
Maheswaran, M., and Casinelli, J. P. 1992, ApJ, 386,695
Naito, T., and Takahara, F. 1994, J. Phys. G, 20, 477
Ormes, J. F., and Freier, P. S. 1978, ApJ, 222, 471
Ostrowski, M. 1988, A&A, 206, 169
Pajot-el-Abed, P., Melikidze, G., and Tagger, M. 1992, A&A, 257, L9
Pantellini, F. G. E., Heron, A., Adam, J. C., and Mangeney, A. 1992, J. Geophys. Res., 97, 1303
Prandtl, L. 1925, Z. Angew. Math. Mech., 5, 136
Rachen, J., and Biermann, P. L. 1992, in Particle Acceleration in Cosmic Plasmas, ed. G. P. Zank and T. K. Gaisser (New York, AIP), p. 393
Raymond, J. 1991, PASP, 103, 781
Reynolds, S. P. 1988, in Galactic and Extragalactic Radio Astronomy, ed. G. L. Verschurr and K. I. Kellermann (New York, Springer), p. 439
Reynolds, S. P., and Ellison, D. C. 1992, ApJ, 399, L75
Reynolds, S. P., and Ellison, D. C. 1993, Proceedings of the 23rd International Cosmic-Ray Conference, Calgary, Invited, Rapporteur, and Highlight Papers (Singapore, World Scientific), 2, 227
Reynolds, S. P., and Fulbright, M. S. 1990, Proceedings of the 21st International Cosmic-Ray Conference (Adelaide, Univ. of Adelaide), 4, 72
Roger, R. S., and Landecker, T. L., ed. 1988, Supernova Remnants and the Interstellar Medium (Cambridge, Cambridge University Press)
Simpson, J. A. 1983, Ann. Rev. Nucl. Part. Sci., 33, 323
Smith, R. C., Raymond, J. C., and Laming, J. M. 1994, ApJ, 420, 286
Swordy, S. P., Muller, D., Meyer, P., L'Heureux, J., and Grunsfeld, J. M. 1990, Proceedings of the 21st International Cosmic-Ray Conference (Adelaide, Univ. of Adelaide), 3, 93
Swordy, S. P. 1993, Proceedings of the 23rd International Cosmic-Ray Conference, Calgary, Invited, Rapporteur, and Highlight Papers (Singapore, World Scientific), p. 243
van der Laan, H. 1962, MNRAS, 124, 125
Völk, H. J., and Biermann, P. L. 1988, ApJ, 333, L65
Wefel, J. P. 1981, in Origin of Cosmic Rays, IAU Symposium No. 94, ed. G. Setti, G. Spada, and A. W. Wolfendale (Dordrecht, Reidel), p. 39
Wefel, J. P. 1991, in Cosmic Rays, Supernovae, and the Interstellar Medium, ed. M. M. Shapiro, R. Silberberg and J. P. Wefel (Dordrecht, Kluwer), p. 29